The Effect of Clouds and Rain on the Aquarius Salinity Retrieval

Frank J. Wentz

1. Radiative Transfer Equations

At 1.4 GHz, the radiative transfer model for cloud and rain is considerably simpler than that required at higher frequencies. The radiation wavelength (21 cm) is much larger than the rain-drop diameter (≈ mm), and the Rayleigh scattering approximation is valid for specifying the absorption coefficient α_{liq} for liquid water.

$$\alpha_{liq} = a_{ray}\rho_{liq} \tag{1}$$

where ρ_{liq} is the combined density of cloud water and rain water (volume of total water per unit volume of air) and a_{ray} is the Rayleigh coefficient given by

$$a_{ray} = \frac{6\pi}{\lambda}\,\mathrm{Im}\left(\frac{1-\varepsilon}{2+\varepsilon}\right) \tag{2}$$

where λ is the radiation wavelength, ε is the complex dielectric constant of water, and Im(···) denotes taking the imaginary part of the argument. At a frequency of 1.4 GHz and a temperature 5°C, $a_{ray} = 3.78\times10^{-4}$ mm^{-1}. The Rayleigh coefficient has a significant inverse dependence on temperature. Going from 15°C to 0°C, a_{ray} increases by 50%.

The upwelling brightness temperature measured at the top of the atmosphere is given by

$$T_B = T_{Bup} + \tau\left[ET_S + (1-E)\left(T_{Bdown} + \tau T_{Bspace}\right) + (1-E)\Omega T_{Bdown}\right] \tag{3}$$

where T_{Bup} and T_{Bdown} are the upwelling and downwelling brightness temperature contributions just due to the atmosphere, τ is the total atmospheric transmission, E is the sea-surface emissivity, T_S is the sea-surface temperature, and T_{Bspace} is the brightness of space (cosmic background plus galactic). The term Ω accounts for downwelling radiation that is scattered upward, rather than specularly reflected, into the viewing direction. It is a small term relative to the other terms.

The atmospheric quantities T_{Bup}, T_{Bdown}, and τ are computed by integrating through the atmosphere [*Wentz,* 1997]. The integrals involve the vertical profiles of temperature, pressure, water vapor density, and liquid water density ρ_{liq}. Due to the fact that the absorption coefficient α_{liq} is extremely small at 1.4 GHz (as compared to unity), it can be shown that an excellent approximation for the increase in T_B due to the presence of clouds and rain is the following:

$$\Delta T_{B,liq} = 2(1-E)\sec\theta_i \int_0^{H_R} dh\, T_{liq}(h)\,\alpha_{liq}(h) \tag{4}$$

where the integral goes vertically up from the surface (h = 0) to the top of the rain cloud (h = H_R). The term $T_{liq}(h)$ is the temperature of the liquid water. The angle θ_i is the Earth incidence angle, and the term $\sec\theta_i$ accounts for the fact that the viewing path is longer than the vertical distance H_R. Doing the integration and setting the temperature and absorption coefficients to effective values gives

$$\Delta T_{B,liq} = 2(1-E)\overline{T}_{liq}\overline{a}_{ray}L\sec\theta_i \tag{5}$$

where L is the total columnar content of liquid water found by vertically integrating the liquid water content for the surface to the top of the rain cloud.

$$L = \int_0^{H_R} dh\rho_{liq} \tag{6}$$

The terms $\overline{T}_{liq}$ is the averaged temperature of the rain cloud and $\overline{a}_{ray} = a_{\text{ray}}(\overline{T}_{liq})$. Equation (5) shows that the increase in brightness temperature due to cloud and rain is simply proportional to the total content of liquid water in the field of view.

2. Calculation of Liquid Water Content from AMSR-E

This section is based on the cloud/rain retrieval algorithm described by *Wentz and Spencer* [1998]. This algorithm provides an estimate of both cloud water L_C (mm) and rain rate R (mm/h). Assuming a Marshall and Palmer drop size distribution and a uniform terminal velocity, the liquid water content for the rain L_R (mm) is given by:

$$L_R = 0.078H_R R^{0.856} \tag{7}$$

where H_R (km) is the rain column height. The rain-rate retrieval is parameterized in terms a columnar rain rate R_C defined as

$$R_C = RH_R \tag{8}$$

This parameterization is based on the fact that R_C is more directly related to the brightness temperature observation than is R. In the Wentz and Spencer algorithm, R_C is the actual retrieved parameter, and (8) is used to convert it to a surface rain rate. Combining (7) and (8) shows that the calculation of L_R is only weakly dependent on the specification of H_R.

$$L_R = 0.078H_R^{-0.144}R_C^{0.856} \tag{9}$$

The rain cloud height is assumed to be a simple function of sea-surface temperature.

$$\begin{aligned} H_R &= 1 && T_S < 0 \\ H_R &= 0.14T_S - 0.0025T_S^2 && 0 \le T_S \le 28 \\ H_R &= 2.96 && T_S > 28 \end{aligned} \tag{10}$$

The total liquid water is then

$$L = L_C + L_R \tag{11}$$

Figure 1 shows a daily map of L for January 1, 2004 as derived from AMSR-E. Only the ascending orbit segments are shows. As can be seen, L reaches maximum values of 2 mm or greater in areas of heavy rain.

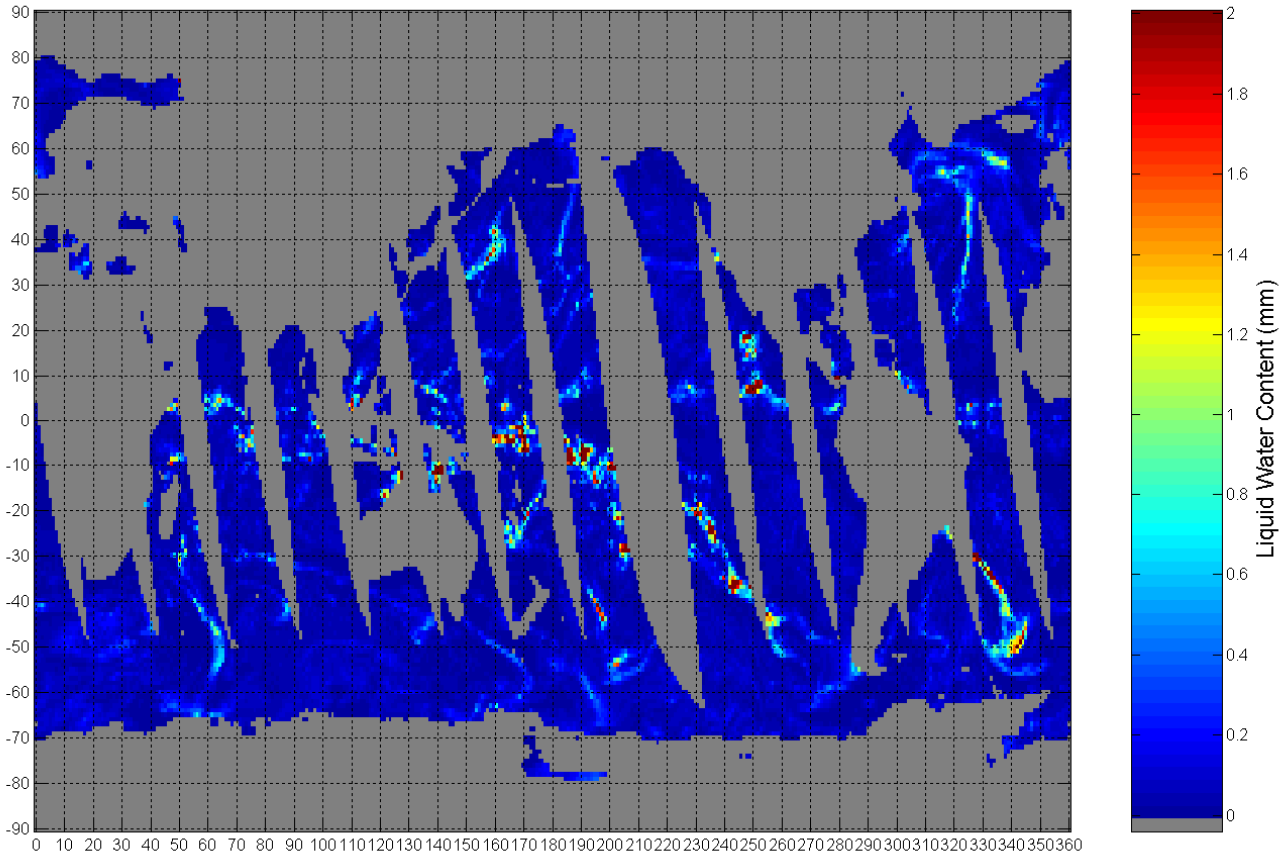

Figure 1. Total atmospheric liquid water (both cloud and rain) as derived by AMSR-E on January 1, 2004. Only the results for the ascending orbits are shown. Liquid water has first been averaged into 1° latitude-longitude bins before displaying.

As mentioned above, the columnar rain rate R_C is the more basic observable for microwave radiometers as compared to surface rain rate R. In fact, it can be shown that the rain retrieval algorithm can be parameterized directly in terms of L rather than R or R_C. The retrieval of L is more robust than that for R because it is less dependent on assumptions regarding the rain column height and the partitioning of cloud water and rain water. Therefore, an accurate estimation of L does not require that rain rate be retrieved. However, since surface rain rate is a familiar parameter, it is informative in a qualitative sense to show how the 1.4 GHz brightness temperature increases with R. Figure 2 shows this relationship. The particular shape to the curve is due to the details of the cloud and rain relationships given in *Wentz and Spencer* [1998].

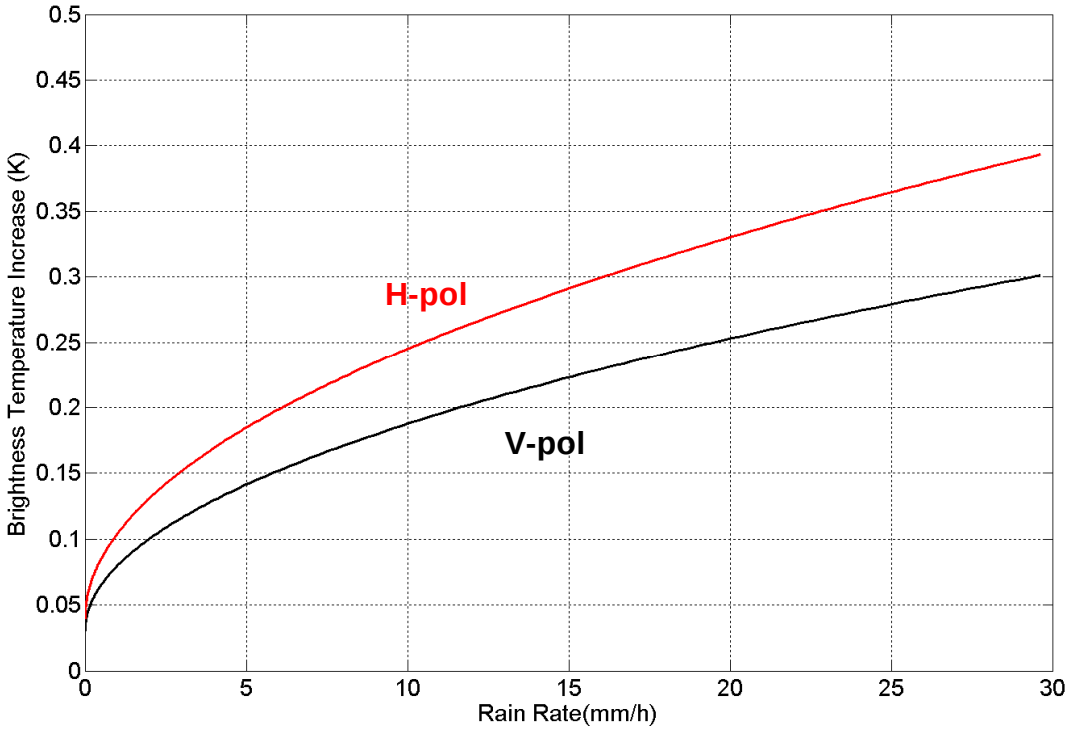

Figure 2. The increase in the 1.4 GHz brightness temperature versus rain rate assuming an incidence angle of θ_i = 45°.

3. Simulation of Aquarius Errors Resulting from Liquid Water

The liquid water retrievals from AMSR-E are converted into a brightness temperature increase at 1.4 GHz using equation (5). In addition to L, the $\Delta T_{B,liq}$ calculation requires the specification of the sea-surface emissivity E and the average temperature of the liquid water $\overline{T}_{liq}$. The emissivity E is found by assuming a specular emissivity with the dielectric constant given by the *Meissner and Wentz* [2004] model (which is similar to the Klein-Swift model). Surface roughness has a completely negligible effect on the calculation of$\Delta T_{B,liq}$. The specular emissivity is a function of surface temperature T_S and sea-surface salinity S. T_S is found from the Reynolds' weekly SST product that is interpolated in time and space to the location of the AMSR-E observation. The salinity is set to a constant value of 35 psu. The liquid water temperature is specified by assuming a mean cloud height of 2 km above the sea surface and a typical atmospheric lapse rate. This allows us to specify a $\overline{T}_{liq}$ versus T_S relationship.

Once $\Delta T_{B,liq}$ is computed for both v-pol and h-pol, an equivalent salinity retrieval error can be found from our basic salinity retrieval algorithm:

$$\hat{S} = a_0(T_S,\theta_i) + a_1(T_S,\theta_i)T_{BV} + a_2(T_S,\theta_i)T_{BH} + a_3(T_S,\theta_i)\hat{W} \tag{12}$$

where the coefficients a_i are known functions of T_S and incidence angle θ_i, and $\hat{W}$ is our best estimate of wind speed. The salinity error due to liquid water is then

$$\Delta\hat{S}_{liq} = a_1\left(T_S,\theta_i\right)\Delta T_{BV,liq} + a_2\left(T_S,\theta_i\right)\Delta T_{BH,liq} \tag{13}$$

The quantities $\Delta T_{BV,liq}$, $\Delta T_{BH,liq}$, and $\Delta\hat{S}_{liq}$ are found for the month of January 2004. Table 1 provides the mean and standard deviation for each error. The error has a small dependence on incidence angle. The longer path through the atmosphere that occurs at the higher incidence angles causes the error to increase. The value of θ_i for horns 1, 2, and 3 are 29.2°, 37.9°, and 45.5°, respectively.

Table 1. Statistics on Errors Resulting from Liquid Water in the Atmosphere.

	Num. Obs.	$\Delta T_{BV,liq}$ Mean (K)	$\Delta T_{BV,liq}$ Std. Dev. (K)	$\Delta T_{BH,liq}$ Mean (K)	$\Delta T_{BH,liq}$ Std. Dev. (K)	$\Delta\hat{S}_{liq}$ Mean (psu)	$\Delta\hat{S}_{liq}$ Std. Dev. (psu)
Inner Horn	**1573473**	**0.018**	**0.030**	**0.020**	**0.033**	**0.041**	**0.065**
Middle Horn	**1573473**	**0.019**	**0.032**	**0.022**	**0.038**	**0.042**	**0.067**
Outer Horn	**1573473**	**0.020**	**0.034**	**0.026**	**0.044**	**0.044**	**0.069**

The errors are further characterized by showing their normalized histogram and their cumulative distribution function in Figures 3 and 4. (The histograms are normalized by their maximum value.) The results shown in these figures are for Aquarius' outer horn.

Similar statistics are done for July 2004, and the results are about the same as for January 2004.

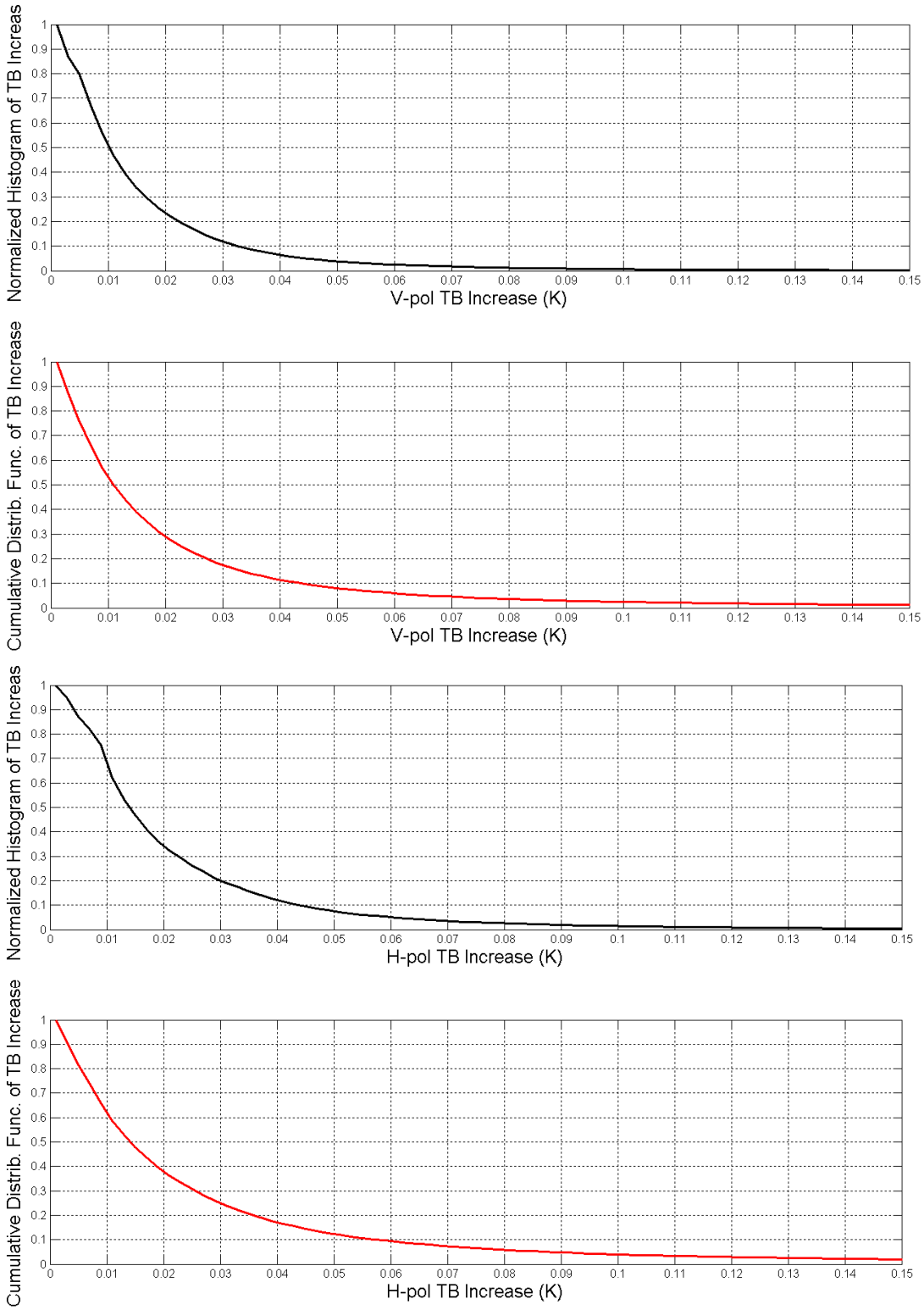

Figure 3. The normalized histogram and cumulative distribution function for the increase in the v-pol brightness temperature (top 2 plots) and the h-pol brightness temperature (bottom 2 plots).

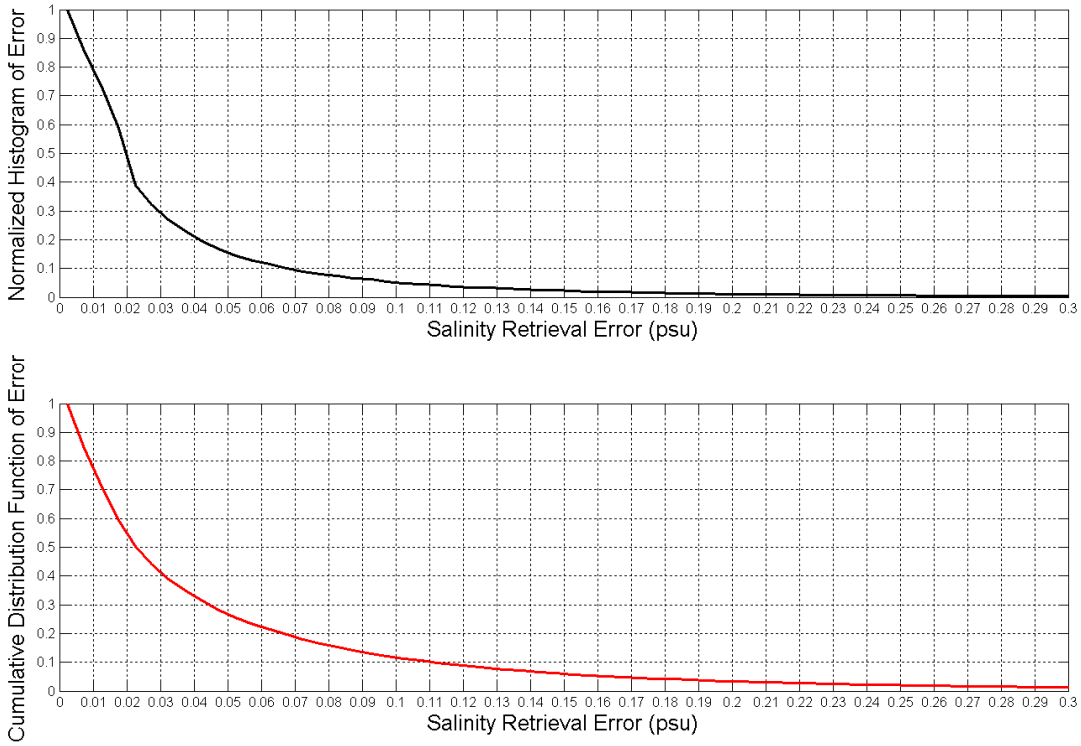

Figure 4. The normalized histogram and cumulative distribution function for the error in the salinity retrieval.

The above statistics tend to understate the potential problem of atmospheric liquid water. The problem can be more clearly seen in Figures 5, 6 and 7 that show the AMSR-E results for one day: January 1, 2004. These figures is very similar to the liquid water map shown in Figure 1 except that L has been mapped into the brightness temperature increase at 1.4 GHz ($\Delta T_{BV,liq}$, $\Delta T_{BH,liq}$) and salinity retrieval error ($\Delta \hat{S}_{liq}$). Salinity errors exceeding 0.1 psu are common within rain systems. The cumulative distribution function in Figure 4 shows that the salinity error exceeds 0.1 psu for 11% of the observations.

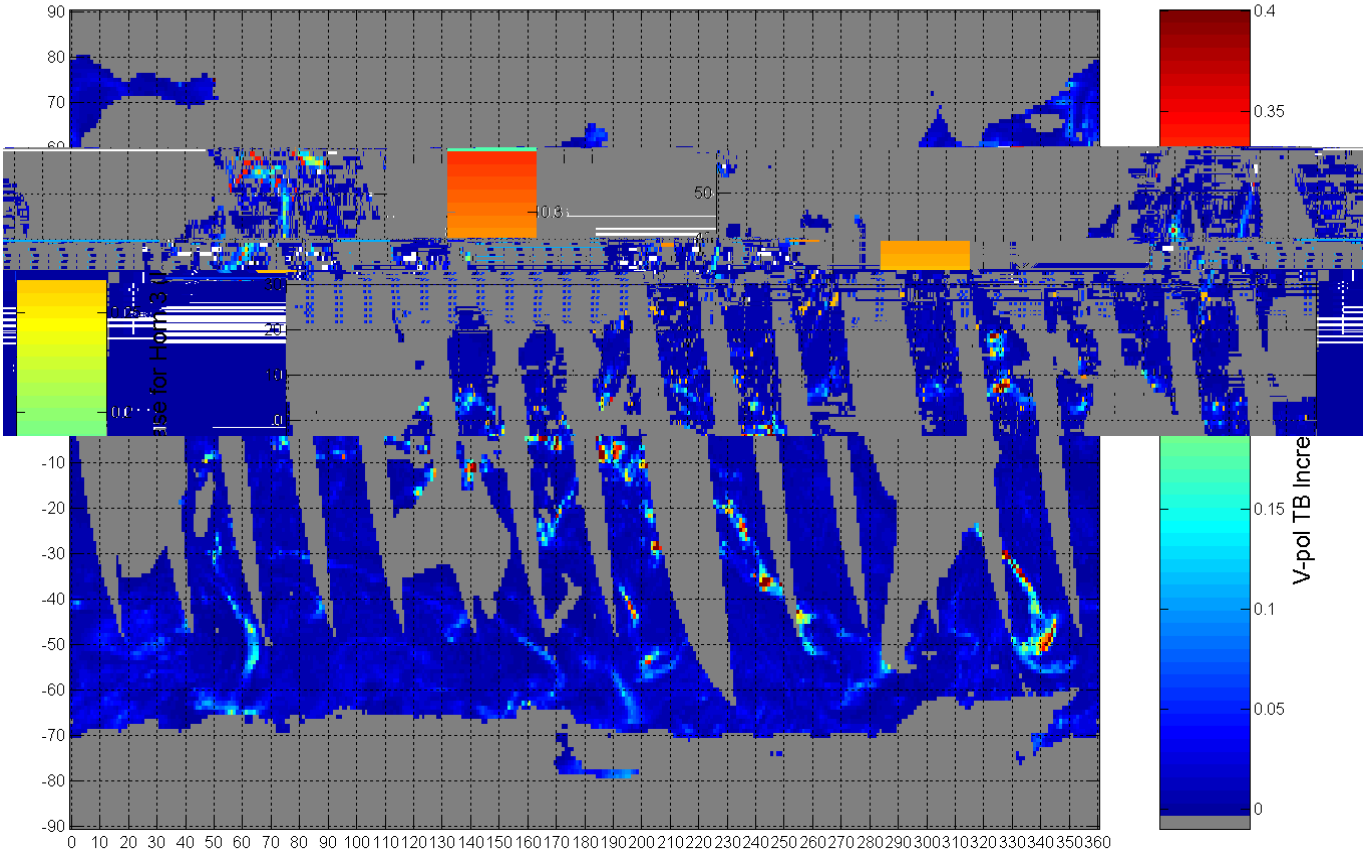

Figure 5. The simulated increase in the 1.4 GHz v-pol brightness temperatures due to atmospheric liquid water derived from the AMSR-E observations for January 1, 2004. Only the results for the ascending orbits are shown. The observations are at a 1°-latitude by 1°-longitude spatial resolution.

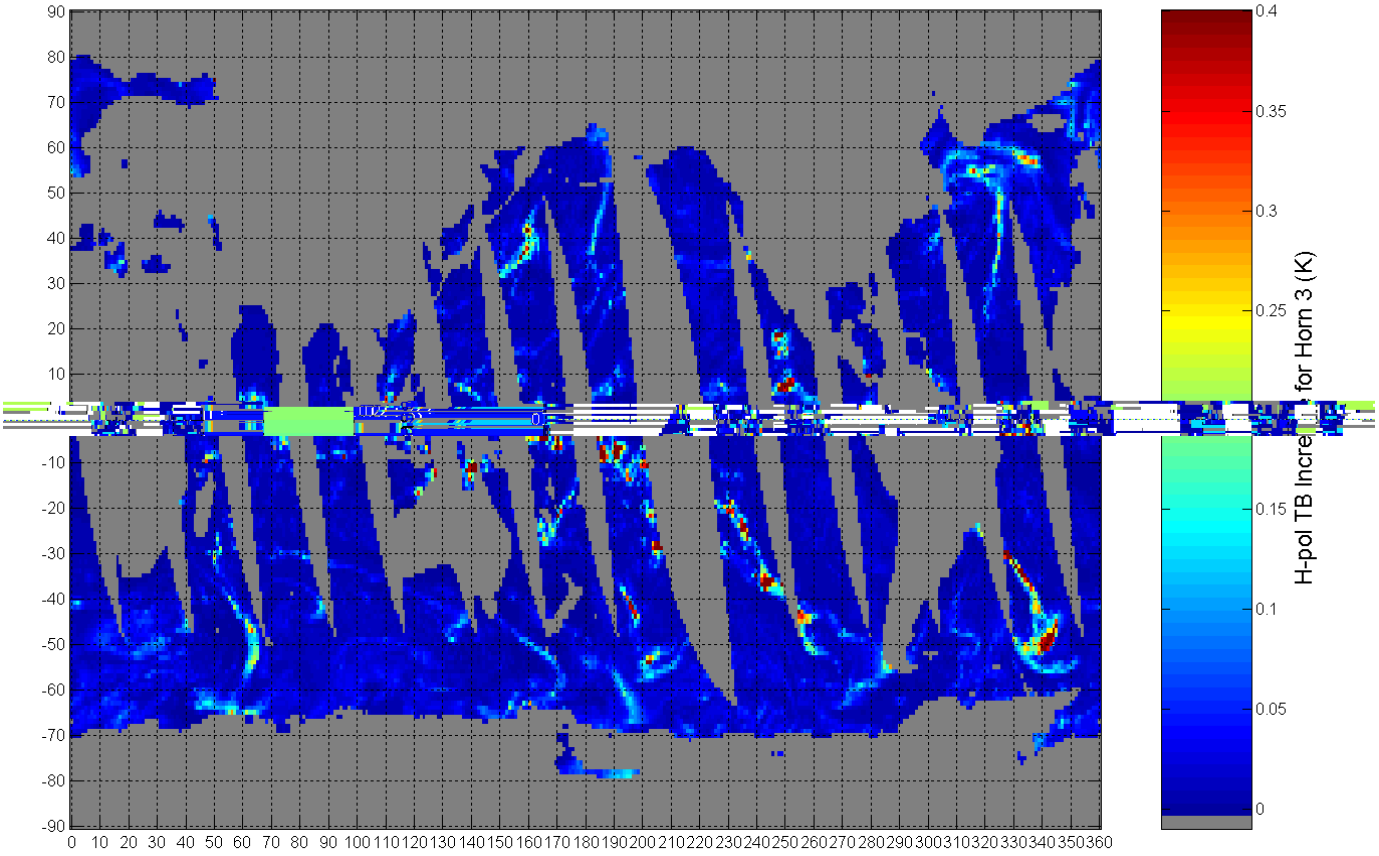

Figure 6. Same as Figure 5 except that the h-pol brightness temperature is shown.

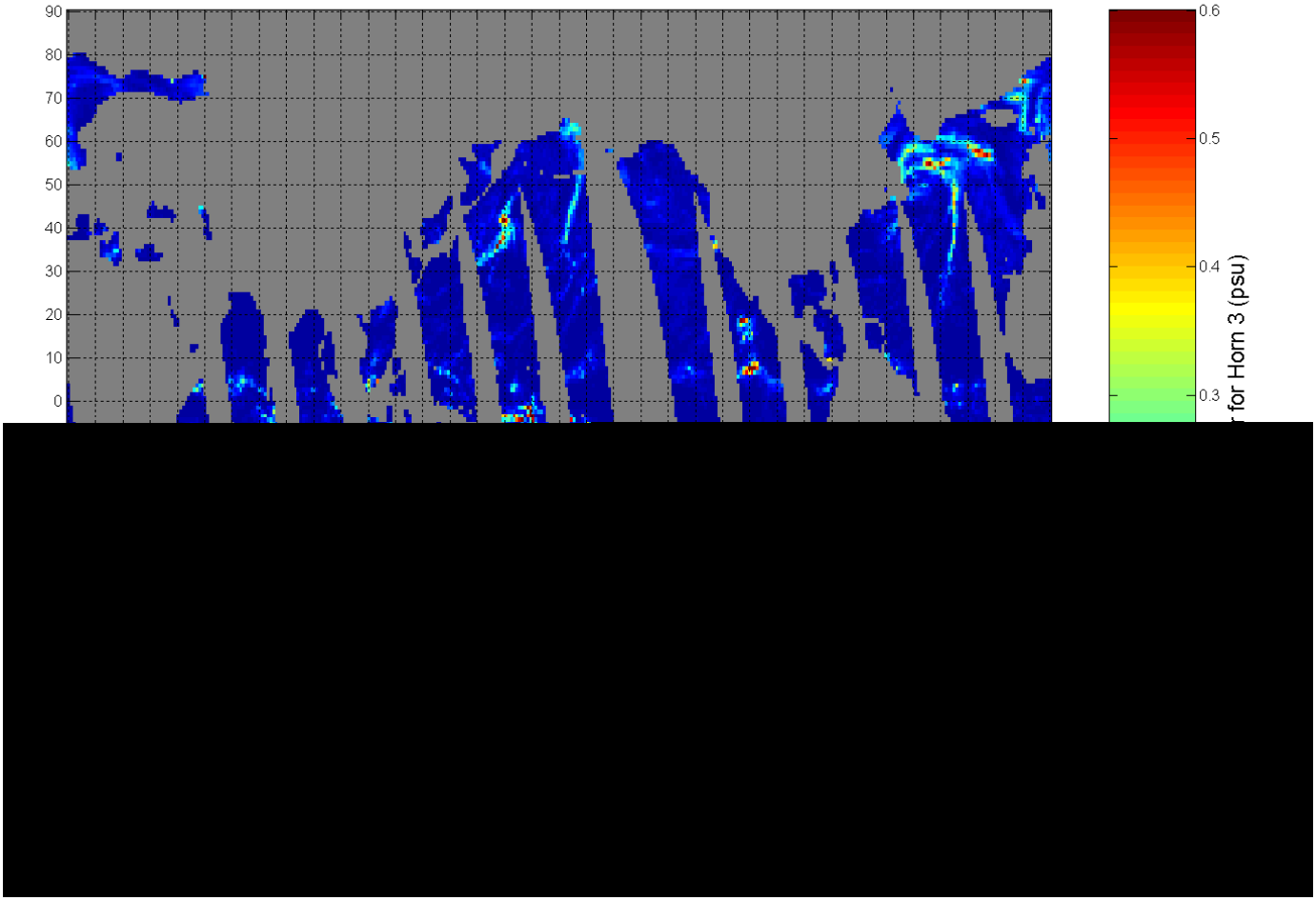

Figure 7. Same as Figure 5 except that the salinity error is shown.

4. Discussion

The overall error in salinity retrievals due to atmosphere liquid water is about 0.07 to 0.08 psu. Although this average global error is relatively small, its real impact is that it is spatially correlated with rain systems and can become quite large in areas of intense rain. About 11% of the Aquarius observations will have a salinity error greater than 0.1 psu if no flagging or correction procedure is implemented.

With respect to flagging and correcting areas having large liquid water contents, there are three options:

1. Aquarius will have a 23/37 GHz radiometer onboard that is collocated with the 1.4 GHz salinity observations. If this radiometer operates successfully, it will provide an ideal tool for flagging and correcting observations that are affect by large L values. For this application, the requirements on the 23/37 GHz radiometer calibration are not very stringent. The radiometer only needs to be stable over time scales of 10-minutes to measure the contrast between rain and no-rain scenes. Furthermore, this T_B contrast only needs to be measured to an accuracy of a few Kelvin. These requirements are well within the design goals of the 23/37 GHz radiometer.

2. The Defense Meteorological Satellite Program (DMSP) will be flying the operational SSM/IS microwave radiometer in an orbit similar to Aquarius. The SSM/IS is capable of making very accurate measurements of the total liquid water. We are currently obtaining information on the planned DMSP ascending node times so that we can access the collocation geometry between SSM/IS and Aquarius.

3. The Global Precipitation Mission (GPM) will be producing daily maps of global precipitation from multiple satellites. These daily maps could be used to flag and correct areas of moderate-to-heavy rain.

We have done some preliminary investigations on the possibility of correcting the salinity retrievals in areas of high L rather than just flagging them. Due to the fact that at L-band the radiative transfer equations simply depend on L (rather than factors like drop-size distribution, radiative scattering, and rain cloud height), a liquid water correction is certainly feasible. The primary requirement is to obtain an accurate estimate of L at spatial scales near 100 km. Collocation issues not withstanding, we expect that L can be estimated to an accuracy of about 25% from satellite microwave radiometers operating in the 18-37 GHz band. This 25% accuracy is based on results coming from the GPM community from which accuracies of 25% to 40% are being reported for microwave rain rate retrievals. The estimation of L at a 100-km resolution is considerably easier than surface rain rate at 25-km resolution, so a 25% error on L seems reasonable. However, to achieve this will require a detailed investigation using satellite data at multiple frequencies. For example, we have completed a very preliminary study based on AMSR-E. The AMSR-E observations at 19-37 GHz are used to estimate L as described herein, and then this estimate of L is used to predict the increase in the 6.9 and 10.7 GHz brightness temperatures. The predicted T_B increase is compared to the observed increase in areas of moderate to heavy rain, and the agreement suggests the accuracy of L is better than 25%.

If the Aquarius 23/37 GHz radiometer operates marginally well and/or if the DMSP SSM/IS flies in an orbit overlapping Aquarius, then accurate collocation will be achievable. Given good collocation and a 25% accuracy on the estimate L, a correction will be possible that reduces the impact of L by a factor of 4, at least for liquid water contents up to about 2 mm (about 6 mm/h

rain rate). For higher rain rates, our ability to estimate L will degrade and flagging may be the better option. At a spatial resolution of 100 km, the AMSR-E data show that observations for which $L > 2$ mm occur only 0.2% of the time. The salinity error for the remaining 99.8% of the observations after correcting for L is about 0.02 psu. A map of the salinity error for this scenario is shown in Figure 8.

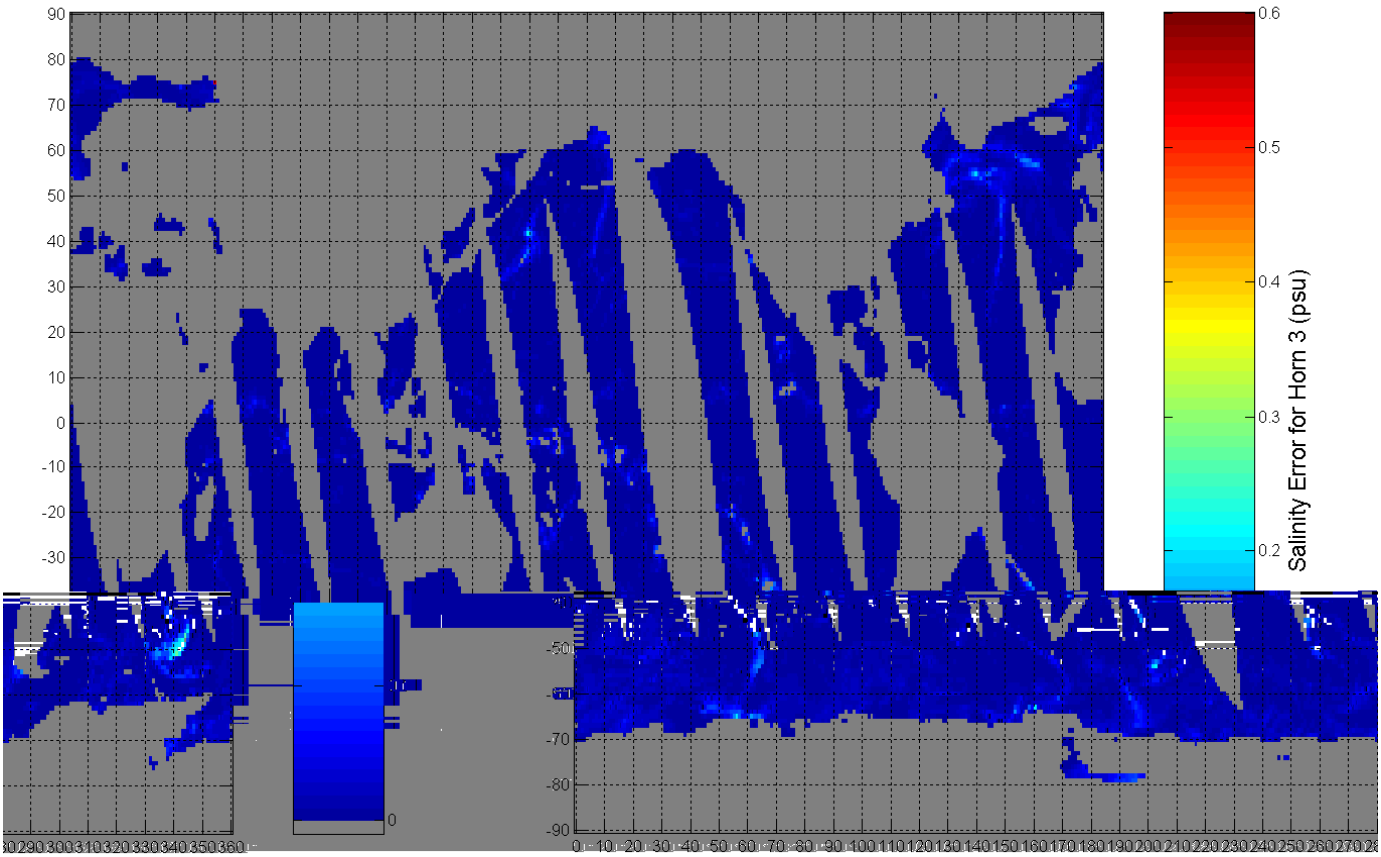

Figure 8. The salinity retrieval error assuming that *L* can be estimated to an accuracy of 25%. Observations for which *L* > 2 mm are discarded. The area of high salinity errors in the South Atlantic could be removed by decreasing the *L* cutoff from 2 mm to 1 mm. The 2-mm cutoff removes 0.2% of the observations, whereas a 1-mm cutoff would remove 0.9% of the observations.

5. References

Wentz, F.J., A well calibrated ocean algorithm for special sensor microwave / imager, *Journal of Geophysical Research, 102* (C4), 8703-8718, 1997.

Wentz, F.J., and R.W. Spencer, SSM/I rain retrievals within a unified all-weather ocean algorithm, *Journal of the Atmospheric Sciences, 55* (9), 1613-1627, 1998.

Meissner, T. and F.J. Wentz, The Complex Dielectric Constant of Pure and Sea Water from Microwave Satellite Observations, *IEEE Transactions on Geoscience and Remote Sensing, 42(9)*, 1838-1849, 2004.

Appendix: Math Notes (for internal use)

Derivation of Equation (5) :

$$T_B = T_X\left(1-\tau^2 R\right)$$

$$\tau^2-\tau_r^2=\left(\tau+\tau_r\right)\left(\tau-\tau_r\right)\approx 2\tau\left(\tau-\tau_r\right)=2\tau^2\left(1-\frac{\tau_r}{\tau}\right)=2\tau^2\left(1-e^{-A_L L\sec\theta}\right)$$

$$\Delta T_B = 2RT_X\tau^2\left(1-e^{-A_L L\sec\theta}\right)\approx 2RT_X\tau^2 A_L L\sec\theta\approx 2RT_X A_L L\sec\theta$$

$$=2\left(1-E\right)\overline{T}_{liq}\overline{a}_{ray}L\sec\theta_i$$